

Electronic Griffiths Phase of the $d = 2$ Mott Transition

E. C. Andrade,^{1,2} E. Miranda,² and V. Dobrosavljević¹

¹*Department of Physics and National High Magnetic Field Laboratory, Florida State University, Tallahassee, Florida 32306, USA*

²*Instituto de Física Gleb Wataghin, Unicamp, Caixa Postal 6165, Campinas, São Paulo 13083-970, Brazil*

(Received 6 August 2008; published 20 May 2009)

We investigate the effects of disorder within the $T = 0$ Brinkman-Rice scenario for the Mott metal-insulator transition in two dimensions. For sufficiently weak disorder the transition retains the Mott character, as signaled by the vanishing of the local quasiparticle weights Z_i and strong screening of the renormalized site energies at criticality. In contrast to the behavior in high dimensions, here the local spatial fluctuations of quasiparticle parameters are strongly enhanced in the critical regime, with a distribution function $P(Z) \sim Z^{\alpha-1}$ and $\alpha \rightarrow 0$ at the transition. This behavior indicates a robust emergence of an electronic Griffiths phase preceding the metal-insulator transition, in a fashion surprisingly reminiscent of the “infinite randomness fixed point” scenario for disordered quantum magnets.

DOI: 10.1103/PhysRevLett.102.206403

PACS numbers: 71.10.Fd, 71.10.Hf, 71.23.-k, 71.30.+h

The effects of disorder on quantum criticality [1] prove to be much more dramatic than in classical systems. Here, some critical points can be described by an “infinite randomness fixed point” (IRFP) [2] and the associated quantum Griffiths phase. Such exotic behavior is well established in insulating quantum magnets with discrete internal symmetry of the order parameter [3], but may or may not survive in other models or in the presence of dissipation due to conduction electrons.

More general insight into the robustness of the IRFP scenario rests on a recently proposed symmetry classification [1], based on the lower critical dimension of droplet excitations. These ideas have found support in very recent work [4], sparking considerable renewed interest [5]. Much of this progress, however, relies on the ability to identify an appropriate order parameter, describing the corresponding symmetry breaking transitions.

The metal-insulator transition (MIT) represents another important class of quantum criticality, one that often cannot be reduced to breaking any static symmetry. Conventional theories of the MIT in disordered systems [6], based on the diffusion mode picture, strongly resemble standard critical phenomena and thus do not easily allow [3] for rare event physics or IRFP behavior. There currently exists, however, a large body of experimental work [7], documenting disorder-induced non-Fermi-liquid behavior due to rare disorder configurations, even in systems far from any spin or charge ordering.

Theoretically, such “electronic Griffiths phases” (EGPs) [8–10] have recently been proposed for correlated electronic systems with disorder, based on generalized dynamical mean-field theory (DMFT) approaches [3,11]. All these works were performed on the Bethe lattice and identified EGPs only in the vicinity of disorder-driven MITs, in particular, only for strong enough disorder, in contrast to quantum magnets where even weak disorder often results in IRFP behavior. Some key unanswered

questions thus remain: (a) What is the effect of weak to moderate disorder on interaction-driven MITs such as the Mott transition in finite dimensions? (b) Is the critical behavior dramatically changed as in the examples of IRFP or may a more conventional scenario suffice?

In this Letter, we investigate the effects of weak and moderate disorder on the Mott MIT at half filling [12] in two dimensions. As the simplest description of the effects of disorder on the Mott transition, we work within a Brinkman-Rice (BR) scenario [13], where a Gutzwiller variational approximation is applied to a disordered two-dimensional Hubbard model. Our results demonstrate that (i) for sufficiently weak disorder the transition retains the second order Mott character, where electrons gradually turn into localized magnetic moments; (ii) disorder-induced spatial inhomogeneities give rise to an intermediate EGP that displays IRFP character at criticality, even when the transition is approached by increasing the interaction at weak disorder; (iii) the renormalized disorder seen by quasiparticles is strongly screened only at low energies, resulting in pronounced energy-resolved inhomogeneity of local spectral functions.

Model.—We focus on the paramagnetic disordered Hubbard model with nearest-neighbor hopping and with site energies ε_i uniformly distributed in the interval $[-W/2, W/2]$ [10,14]. We approach the Mott transition by increasing the on-site Hubbard interaction U at half filling (chemical potential $\mu = U/2$), on an $L \times L$ square lattice with periodic boundary conditions. All energies will be expressed in units of the clean Fermi energy (half-bandwidth) $E_F = 4t$, where t is the hopping amplitude.

Within our disordered BR approach, we self-consistently calculate the local single-particle self-energies $\tilde{\Sigma}_i(\omega_n)$ [10,14], which assume a site-dependent form

$$\tilde{\Sigma}_i(\omega_n) = (1 - Z_i^{-1})\omega_n + v_i - \varepsilon_i + \mu. \quad (1)$$

The renormalized site energies $v_i = v_i(e_i, d_i)$ and the local

quasiparticle (QP) weights $Z_i = Z_i(e_i, d_i)$ are variationally calculated through the saddle-point solution of the corresponding Kotliar-Ruckenstein slave boson functional [15]

$$F = -2T \sum_{\omega_n} \text{Tr} \ln[-i\omega_n \mathbf{1} + \mathbf{Z}\mathbf{v} + \mathbf{Z}^{1/2} \mathbf{H}_0 \mathbf{Z}^{1/2}] + \sum_i [Ud_i^2 - (1 - e_i^2 + d_i^2)(Z_i v_i - \varepsilon_i + \mu)]. \quad (2)$$

Here, e_i and d_i are the Kotliar-Ruckenstein slave boson amplitudes [15], T is the temperature, and ω_n are the Matsubara frequencies. The operators \mathbf{Z} and \mathbf{v} are site-diagonal matrices $[\mathbf{Z}]_{ij} = Z_i \delta_{ij}$ and $[\mathbf{v}]_{ij} = v_i \delta_{ij}$, and \mathbf{H}_0 is the clean and noninteracting lattice Hamiltonian.

This approach is mathematically equivalent to a generalization of the DMFT [11] to finite dimensions, the ‘‘statistical DMFT’’ [10] implemented using a slave boson impurity solver, which provides an elegant and efficient computational approach, allowing us, for example, to calculate Z_i values spanning 8 orders of magnitude. We considered several lattice sizes ranging up to $L = 50$, and for every (U, W) pair we typically generated around 40 realizations of disorder. We carefully verified that for such large lattices, all our results are robust and essentially independent of the system size (see, e.g., the inset of Fig. 2).

Phase diagram and Griffiths phase.—To characterize the $T = 0$ disordered Mott transition in $d = 2$, we follow the evolution of the local QP weights Z_i , as the interaction U is increased at fixed disorder W . For weak to moderate disorder, we find behavior partly reminiscent of that previously established for high dimensions (‘‘DMFT limit’’) [16]. The approach to the critical point at $U = U_c(W)$ is identified by the vanishing of the typical QP weight $Z_{\text{typ}} = \exp\{\langle \ln Z_i \rangle\}$ [10], indicating the Mott transmutation of a finite (large) fraction of electrons into local magnetic moments. Because random site energies tend to push the local occupation away from half filling, $U_c(W)$ increases with disorder (Fig. 1).

The role of fluctuation effects, however, is best seen by contrasting our $d = 2$ results to those found in the DMFT limit [14]. There each site has many neighbors, and thus ‘‘sees’’ the same (self-averaged) environment (‘‘cavity’’), so $Z_i^{\text{DMFT}} = Z^{\text{DMFT}}(\varepsilon_i)$ depends only on the local site energy ε_i . Its minimum value corresponds to the sites closest to half-filling $Z_{\text{min}}^{\text{DMFT}} \equiv Z_o = Z^{\text{DMFT}}(\varepsilon_i = 0)$. In the critical region all $Z_i^{\text{DMFT}} \sim \langle Z \rangle \sim U_c^{\text{DMFT}}(W) - U$, but the scaled local QP weights $z_i^{\text{DMFT}} = Z_i^{\text{DMFT}}/Z_o$ approach finite values at the transition, with $z_{\text{min}}^{\text{DMFT}} = 1$. The corresponding scaled distribution $P(z_i^{\text{DMFT}})$ approaches a fixed-point form close to $U_c^{\text{DMFT}}(W)$ (shown by the thick solid line in Fig. 2).

In low dimensions, site-to-site cavity fluctuations give rise to a low- Z tail emerging below the DMFT minimum value Z_o (Fig. 2). To bring this out, we present our $d = 2$ results in precisely the same fashion as in the DMFT limit, i.e., scaling each Z_i with Z_o . Away from the transition the

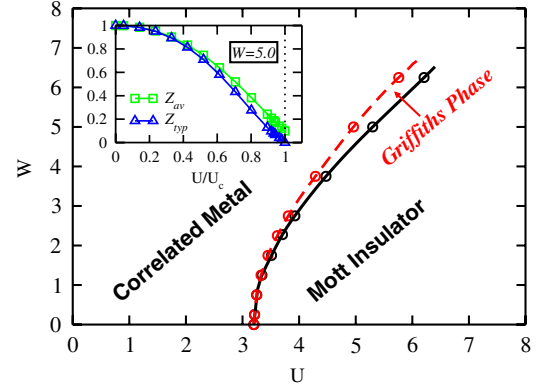


FIG. 1 (color online). $T = 0$ phase diagram of the disordered half-filled Hubbard model in $d = 2$, as a function of the interaction U at weak to moderate disorder strength $W \lesssim U$. An intermediate electronic Griffiths phase emerges separating the disordered Fermi liquid metal and the Mott insulator. The inset shows the typical (Z_{typ}) and average (Z_{av}) values of the local quasiparticle weight Z_i as a function of U . The Mott transition is identified by the (linear) vanishing of Z_{typ} . Note that Z_{av} is finite at U_c , indicating that a fraction of the sites remains nearly empty or doubly occupied.

distribution resembles the DMFT form, but in the critical region the low- z tail assumes a power-law form:

$$P(z) \sim z^{\alpha-1}. \quad (3)$$

Physically, the emergence of a broad distribution of local QP weights Z_i indicates the presence of rare disorder configurations characterized by anomalously low local

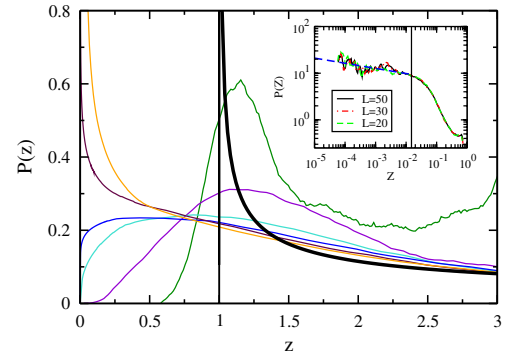


FIG. 2 (color online). Distribution of $z_i = Z_i/Z_o$ (see text) as the transition is approached by increasing U [thin lines correspond to $U/U_c(W) = 0.6, 0.8, 0.9, 0.92, 0.94, 0.97$]. For reference, the thick solid line shows the DMFT ‘‘fixed-point’’ distribution which remains bounded from below. Our $d = 2$ results show that, due to rare events, a low- z tail $P(z) \sim z^{\alpha-1}$ emerges for $z \lesssim 1$ as the transition is approached. In the critical region the distribution assumes a singular form ($\alpha < 1$), indicating the onset of an electronic Griffiths phase. Results are shown for $W = 5.0$ and $L = 20$. The inset illustrates how for such large lattices our results for $P(Z)$ are essentially independent of the system size [shown for $U/U_c(W) = 0.94$ and $\alpha = 0.77 \pm 0.06, 0.81 \pm 0.05, 0.82 \pm 0.05$ corresponding to $L = 20, 30, 50$, respectively].

energy scales $\Delta_i \approx Z_i E_F$. Since the approach to the Mott insulator corresponds to $Z \rightarrow 0$, such regions with $Z_i \ll Z_{\text{typ}}$ should be recognized as “almost localized” Mott droplets. Within our BR picture, each local region provides [10] a contribution $\chi_i \sim \gamma_i \sim Z_i^{-1}$ to the spin susceptibility or the Sommerfeld coefficient, respectively. The local regions with the smallest Z_i thus dominate the thermodynamic response and produce non-Fermi-liquid metallic behavior [8,9] whenever $\alpha < 1$.

IRFP-like behavior.—To carefully calculate the exponent $\alpha(U)$ as the transition is approached, we use two distinct methods. The first relies on the “estimator” [17] $\alpha = \langle \ln[Z_{\text{max}}/Z_i] \rangle_{Z_i \leq Z_{\text{max}}}^{-1}$, where $Z_{\text{max}} \sim Z_{\text{typ}} \sim Z_o$ (see Fig. 2) is an appropriate upper bound on the power-law behavior. The second approach consists in calculating $\langle Z^{-\mu} \rangle_{Z_i \leq Z_{\text{max}}}^{-1}$ for given μ , as a function of U . This quantity is expected to vanish at $U = U_\mu$, satisfying $\alpha(U_\mu) = \mu$. Both methods give consistent results (open and closed symbols, respectively, in Fig. 3), which agree within the estimated error bars.

The exponent α is found to decrease smoothly as the transition is approached, until the distribution assumes a singular form ($\alpha < 1$), indicating the emergence of an EGP [8,9]. Its estimated onset ($\alpha = 1$) is generally found to strictly precede the MIT (dashed line in Fig. 1), indicating that disorder fluctuations qualitatively modify the critical behavior even for weak to moderate disorder. Remarkably, we find that, within our numerical accuracy, $\alpha \rightarrow 0$ precisely along the critical line $U = U_c(W)$. This establishes a phenomenology which closely parallels the behavior of magnetic Griffiths phases with IRFP behavior [1,3].

Structure of the rare events.—To explore the nature of the rare events (REs) dominating the EGP, i.e., the regions with $Z_i \ll Z_{\text{typ}}$, we examined a number of disorder realizations and selected those few samples containing the smallest Z_i . A typical example is shown in Fig. 4, where the RE is seen as a very sharp peak of the local spin

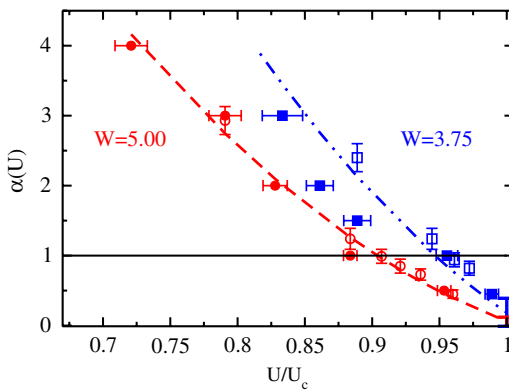


FIG. 3 (color online). Exponent $\alpha(U)$ for two different values of disorder. To calculate α we use two methods (open and closed symbols, see text). Results are shown for $L = 20$. Within the estimated error bars, we find an extrapolated value consistent with $\alpha = 0$ at the critical point $U = U_c(W)$.

susceptibility $\chi_i \sim Z_i^{-1}$ (note the logarithmic scale). The corresponding RE site is then placed in the middle of a box of side l (dashed line in Fig. 4). To examine the spatial correlations, we preserve the same disorder realization within this box, while the outside is replaced by an appropriate DMFT effective medium. We then recalculate the QP parameters Z_i as the box size is reduced from $l = L$ (original model), down to $l = 1$ (DMFT limit where all spatial correlations are suppressed). We find that the RE is essentially unmodified until the box size reaches $l \sim l_{\text{RE}}$ (≈ 9 for the example in Fig. 4), and then is rapidly (exponentially) suppressed for $l < l_{\text{RE}}$. We also find that the variance of the disorder strength within the box of size l_{RE} is appreciably weaker than on the average, establishing that the REs dominating the Griffiths phase stem out from rare disorder configurations, precisely as expected within the IRFP scenario.

Critical behavior of the spatial inhomogeneity.—As $\alpha \rightarrow 0$ in the critical region, the $P(Z_i)$ distribution becomes “infinitely broad,” since α^{-1} measures [3] the variance of $\ln Z_i$. The thermodynamic response becomes increasingly inhomogeneous as the transition is approached; such behavior is typically seen in NMR experiments on materials displaying disorder-driven non-Fermi-liquid behavior [3].

But what to expect from STM experiments directly measuring the local electronic spectra? Within our BR

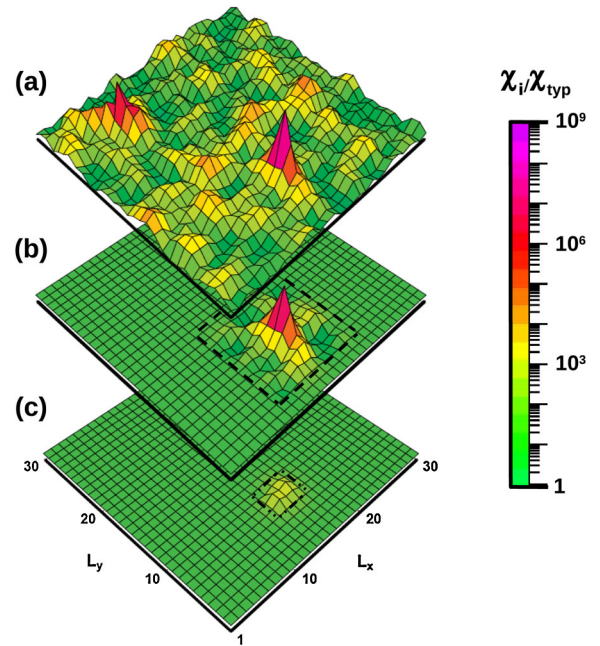


FIG. 4 (color online). (a) Spatial distribution of the (normalized) local spin susceptibilities $\chi_i \sim Z_i^{-1}$, illustrating a typical disorder realization containing a RE with $\chi_i \gg \chi_{\text{typ}}$. (b) Disorder fluctuations are eliminated outside a box of size $l = 9$, without appreciably affecting the RE. (c) When the box is further reduced (here $l = 3$), the RE is rapidly (exponentially) suppressed, establishing the nonlocal nature of the rare event, in strong support of the IRFP picture. Results are shown for $L = 30$, $W = 5.0$, and $U/U_c = 0.96$.

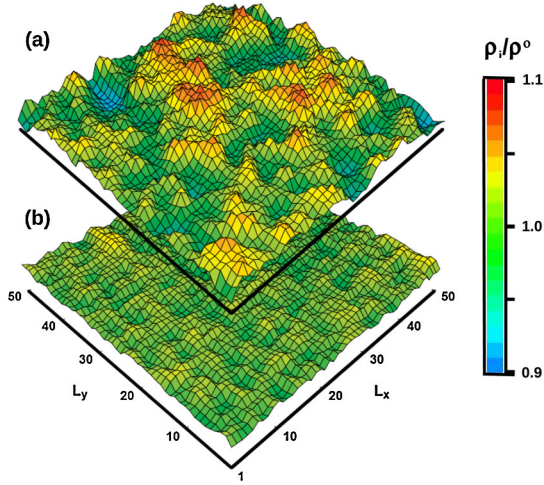


FIG. 5 (color online). Spatial distribution of the local density of states normalized by its clean value, for one disorder realization, shown (a) away from the Fermi energy ($\omega = 0.10$) and (b) at the Fermi energy ($\omega = 0$). Because of static disorder screening, the distribution becomes homogeneous close to the Fermi level, but displays pronounced spatial structures at higher energies. Results are shown for $L = 50$, $U/U_c = 0.96$, and $W = 0.75$.

approach, the local density of states in question, $\rho_i(\omega) = \frac{1}{\pi} \text{Im}G_{ii}(\omega - i0^+)$, depends not only on the local QP weights Z_i but also on the renormalized site energies v_i through

$$G_{ii}(\omega) = [(\mathbf{Z}^{-1}\omega - \mathbf{v} - \mathbf{H}_0)^{-1}]_{ii}. \quad (4)$$

The quasiparticles thus “see” a frequency-dependent effective disorder potential

$$\varepsilon_i^{\text{eff}}(\omega) = v_i - \omega/Z_i. \quad (5)$$

Our explicit calculations find that the renormalized site energies v_i become strongly screened near the transition, giving rise to a very small (but finite) renormalized disorder strength $W_{\text{eff}} = \sqrt{\langle v_i^2 \rangle} \ll 1$ at criticality (e.g., for $W = 5$, $W_{\text{eff}} \approx 0.05$). Near the Fermi energy ($\omega = 0$), we predict the local density of states spectra to appear increasingly homogeneous in the critical region. At higher energies, however, the very broad distribution of local QP weights (essentially local QP bandwidths) creates a very strong effective disorder seen by the quasiparticles, and we expect the system to appear more and more inhomogeneous as criticality is approached. This result is illustrated by explicit computation of the density of states profile (Fig. 5), which is surprisingly reminiscent of recent spectroscopic images on doped cuprates [18]. Our theory, which does not include any physics associated with superconducting pairing, strongly suggests that such energy-resolved inhomogeneity is a robust and general feature of disordered Mott systems.

Conclusions.—We presented the first detailed model calculation investigating the effects of moderate disorder on the Mott metal insulator in two dimensions. Our findings indicate that rare disorder fluctuations may dominate quantum criticality even in the absence of magnetic ordering—an idea that begs experimental tests on a broad class of materials. The Brinkman-Rice scenario we considered, which focuses on local (Kondo-like) effects of strong correlation (while neglecting intersite magnetic correlations), may be relevant only for systems with sufficiently strong magnetic frustration, such as ^3He monolayers adsorbed on graphite [19]. Such a variational approach should be generalized for systems, such as copper oxides, where the intersite superexchange is strong, but this fascinating research direction remains a challenge for future work.

This work was supported by FAPESP through Grant No.04/12098-6 (E.C.A.), CAPES through Grant No. 1455/07-9 (E.C.A.), CNPq through Grant No. 305227/2007-6 (E.M.), and NSF through Grant No. DMR-0542026 (V.D.).

-
- [1] T. Vojta, J. Phys. A **39**, R143 (2006).
 - [2] D. S. Fisher, Phys. Rev. B **51**, 6411 (1995).
 - [3] E. Miranda and V. Dobrosavljević, Rep. Prog. Phys. **68**, 2337 (2005).
 - [4] J. A. Hoyos, C. Kotabage, and T. Vojta, Phys. Rev. Lett. **99**, 230601 (2007).
 - [5] A. Del Maestro, B. Rosenow, M. Muller, and S. Sachdev, Phys. Rev. Lett. **101**, 035701 (2008).
 - [6] P. A. Lee and T. V. Ramakrishnan, Rev. Mod. Phys. **57**, 287 (1985).
 - [7] G. R. Stewart, Rev. Mod. Phys. **73**, 797 (2001).
 - [8] E. Miranda and V. Dobrosavljević, Phys. Rev. Lett. **86**, 264 (2001).
 - [9] D. Tanasković, E. Miranda, and V. Dobrosavljević, Phys. Rev. B **70**, 205108 (2004).
 - [10] V. Dobrosavljević and G. Kotliar, Phys. Rev. Lett. **78**, 3943 (1997).
 - [11] A. Georges, G. Kotliar, W. Krauth, and M. Rozenberg, Rev. Mod. Phys. **68**, 13 (1996).
 - [12] N. F. Mott, *Metal-Insulator Transition* (Taylor and Francis, London, 1990).
 - [13] W. F. Brinkman and T. M. Rice, Phys. Rev. B **2**, 4302 (1970).
 - [14] D. Tanasković, V. Dobrosavljević, E. Abrahams, and G. Kotliar, Phys. Rev. Lett. **91**, 066603 (2003).
 - [15] G. Kotliar and A. E. Ruckenstein, Phys. Rev. Lett. **57**, 1362 (1986).
 - [16] M. C. O. Aguiar, V. Dobrosavljević, E. Abrahams, and G. Kotliar, Phys. Rev. B **71**, 205115 (2005).
 - [17] A. Clauset, C. R. Shalizi, and M. E. J. Newman, arXiv:0706.1062.
 - [18] K. McElroy *et al.*, Science **309**, 1048 (2005).
 - [19] A. Casey, H. Patel, J. Nyéki, B. P. Cowan, and J. Saunders, Phys. Rev. Lett. **90**, 115301 (2003).